Physiological and genetic drivers underpinning canopy development are associated with durum wheat yield in rainfed environments

Yichen Kang[1], Shanice V. Haeften[1], Daniela Bustos-Korts[2], Stjepan Vukasovic[3], Sana Ullah Khan[1], Jack Christopher[4], Karine Chenu[4], Jason A. Able[5], Millicent R. Smith[1,6], Kai P. Voss-Fels[1], Andries B. Potgieter[7], David R. Jordan[8], Andrew K. Borrell[8], Samir Alahmad[1*] and Lee T. Hickey[1*]

[1]Centre for Crop Science, Queensland Alliance for Agriculture and Food Innovation, The University of Queensland, Brisbane, QLD, Australia

[2]Biometris, Wageningen University and Research Centre, Wageningen, Netherlands

[3]Institute of Agronomy and Plant Breeding, Justus Liebig University Giessen, Hesse, Germany

[4]Centre for Crop Science, Queensland Alliance for Agriculture and Food Innovation, The University of Queensland, Toowoomba, QLD, Australia

[5]School of Agriculture, Food & Wine, Waite Research Institute, The University of Adelaide, Urrbrae, SA, Australia

[6]School of Agriculture and Food Sciences, Faculty of Science, The University of Queensland, Gatton, QLD, Australia

[7]Centre for Crop Science, Queensland Alliance for Agriculture and Food Innovation, The University of Queensland, Gatton, QLD, Australia.

[8] Centre for Crop Science, Queensland Alliance for Agriculture and Food Innovation, The University of Queensland, Hermitage Research Facility, Warwick, QLD, Australia

*Correspondence: Samir Alahmad, s.alahmad@uq.edu.au

Lee T. Hickey, l.hickey@uq.edu.au

Abstract

Durum wheat (*Triticum turgidum* L. ssp. *Durum*) is largely grown in rainfed production systems around the world. New cultivars with improved adaptation to water-limited environments are required to sustain productivity in the face of climate change. Physiological traits related to canopy development underpin the production of biomass and yield, as they interact with solar radiation and affect the timing of water use throughout the growing season. Despite their importance, there is limited research on the relationship between canopy development and yield in durum wheat, in particular studies exploring temporal canopy dynamics under field conditions. This study reports the genetic dissection of canopy development in a durum wheat nested-association mapping population evaluated for longitudinal normalized difference vegetation index (NDVI) measurements. Association mapping was performed to identify quantitative trait loci (QTL) for time-point NDVI and spline-smoothed NDVI trajectory traits. Yield effects associated with QTL for canopy development were explored using data from four rainfed field trials. Four QTL were associated with yield in specific environments, and notably, were not associated with a yield penalty in any environment. Alleles associated with slow canopy closure increased yield. This was likely due to a combined effect of optimised timing of water-use and pleiotropic effects on yield component traits, including spike number and spike length. Overall, this study suggests that slower canopy closure is beneficial for durum wheat production in rainfed environments. Selection for traits or loci associated with canopy development may indirectly improve yield and support selection for more resilient and productive cultivars in water limited environments.

Keywords: association mapping, drought, marker-environment interaction, NDVI, phenotyping, water stress

Abbreviations

AUC	area under the curve
BLUE	best linear unbiased estimate
DAS	days after sowing
DTF	days to flowering
FDR	false discovery rate
FGCC	fractional green canopy cover
GS	Zadoks' growth stages
MTA	marker–trait associations
NAM	nested-association mapping
NDVI	normalised difference vegetation index
PC	principal component
PCA	principal component analysis
PH	plant height
QTL	quantitative trait loci
SE	stem elongation
SL	spike length
SN	spike number per unit area
SNP	single nucleotide polymorphism
SS	seedling stage
TL	tillering

Introduction

Durum wheat, or pasta wheat (*Triticum turgidum* L. ssp. *Durum*; 2n = 4x = 28) is an ancient food crop and an important industry in Mediterranean and sub-tropical agricultural regions (Sall *et al.*, 2019). Production is often constrained by drought, during and post anthesis (Loss and Siddique, 1994). This can greatly reduce yield potential by limiting grain number and weight (Gevrek and Atasoy, 2012; Royo *et al.*, 2000). Therefore, traits with phenotypic plasticity are important for increasing crop productivity, as trait plasticity allows for adaptive potential in response to environmental variations (Borrell *et al.*, 2014; Maccaferri *et al.*, 2008; Matesanz *et al.*, 2020; Shavrukov *et al.*, 2017). Traditionally, durum wheat breeders have selected for earlier flowering (Bassi and Nachit, 2019; De Vita *et al.*, 2007; Miralles *et al.*, 2002; Motzo *et al.*, 2010) to minimise the impact of end-of-season drought on reproduction and grain-filling.

In addition to optimising flowering time, canopy traits associated with improved water use efficiency can be targeted. For instance, changes in canopy development (e.g., reduction in leaf size or tillering) provide an advantage under terminal drought conditions by shifting water use from pre- to post-anthesis (Borrell *et al.*, 2014; George-Jaeggli *et al.*, 2017). Limited transpiration rate at high evaporative demand can also conserve water for critical stages later in crop development (Collins *et al.*, 2021). There is a fine balance between water supply and demand in crops and as such, the timing of water availability must be matched with phenological development. Although rapid canopy development can increase light interception (Regan *et al.*, 1997) and reduce soil evaporation (Lopez-Castaneda *et al.*, 1995), if there is insufficient stored soil moisture or in-crop rainfall, excessive canopy size may prematurely deplete soil water and exacerbate terminal drought (Nuttall *et al.*, 2012). Thus, crop performance under drought conditions depends on complex source-sink dynamics between carbohydrate and water balance, where there are trade-offs between stress resilience and yield (Collins *et al.*, 2021; Rodrigues *et al.*, 2019). Given the dynamic nature of the environment, understanding canopy development may help to identify integrative traits that support yield.

Normalized difference vegetation index (NDVI) is used to characterise canopy attributes and is considered a good surrogate for biomass accumulation, canopy cover and plant vigour (Cabrera-Bosquet *et al.*, 2011; Carlson and Ripley, 1997; Mullan and Reynolds, 2010; Xue and Su, 2017). NDVI, computed as the difference between near-infrared reflectance and red absorption divided by their sum, is influenced by leaf chlorophyll content and canopy

79 architecture (Gamon *et al.*, 1995). NDVI can be measured in a non-subjective and efficient
80 manner which facilitates its use at the field level. The generalized NDVI profile captured during
81 the growing season includes: (1) the green-up phase before canopy closure, also known as the
82 exponential phase; (2) the peak canopy cover phase; and (3) the decline phase as leaves senesce
83 (Brown and de Beurs, 2008; Masialeti *et al.*, 2010; Smith *et al.*, 1995; Soltani and Galeshi,
84 2002). Hereafter, the term canopy development refers to the green-up and maximum cover
85 phases.

86 While many studies have used NDVI to characterize canopy dynamics during the senescence
87 phase (Christopher *et al.*, 2016; Christopher *et al.*, 2014; Lopes and Reynolds, 2012; Pinto *et*
88 *al.*, 2016), few have explored canopy development and assessed its impact on yield. In durum
89 wheat, genetic studies have mapped quantitative trait loci (QTL) using NDVI captured at
90 certain developmental stages or specific time-points (Condorelli *et al.*, 2018; Shi *et al.*, 2017).
91 However, NDVI captured at a specific time point does not account for the temporal dynamics
92 of canopy development. This is important to consider, as the correlation between NDVI
93 captured at a specific time-point and yield is strongly dependent on the growth stage (Goodwin
94 *et al.*, 2018; Smith *et al.*, 1995; Teal *et al.*, 2006).

95 Alternatively, NDVI time-series data can be modelled, and features of the growth curve used
96 to study the underlying genetics. In bread wheat and maize, longitudinal growth data has
97 successfully captured trait development over time to reinforce QTL mapping power (Kwak *et*
98 *al.*, 2016; Lyra *et al.*, 2020; Miao *et al.*, 2020; Muraya *et al.*, 2017). Different parameters of
99 the growth curve related to the time period of interest, may be used to describe temporal NDVI
100 dynamics, such as curve threshold values, inflection points and integrals (Bustos-Korts *et al.*,
101 2019; Christopher *et al.*, 2014; Lopes and Reynolds, 2012; Pinto *et al.*, 2016). Considering the
102 many environmental factors that can affect the canopy status, area under the respective curve
103 summarises the cumulative changes and can provide a general assessment of canopy
104 development. The approach is yet to be applied to study canopy development in durum wheat.

105 Understanding the genetics of adaptive traits like canopy development, and their interaction
106 with the environment, is critical to support the development of new cultivars with improved
107 adaptation (Hammer *et al.*, 2020). Using a nested-association mapping population, we reveal
108 the genetic components of canopy development in durum wheat. To gain biological and
109 physiological insights into NDVI time-sequential data, we first explored relationships between
110 NDVI, phenology, canopy cover and features of the growth curve. Secondly, we performed

association mapping using both time-point NDVI and the area under the curve (AUC) for NDVI. Finally, markers associated with canopy development were used in a linear mixed model approach to investigate marker × environment interactions and yield effects across multiple rainfed environments in Australia.

Materials and methods

Plant materials and genotyping

This study examined subsets of a durum wheat nested-association mapping (NAM) population developed at The University of Queensland, as described by Alahmad *et al.* (2019). The NAM population comprised 920 lines (10 families) generated by crossing eight elite lines from ICARDA Morocco (i.e. Fastoz2, Fastoz3, Fastoz6, Fastoz7, Fastoz8, Fastoz10, Outrob4 and Fadda98) as 'founders' to the Australian durum wheat cultivars Jandaroi and DBA Aurora, which served as 'reference' varieties. The founder lines were used as donors for drought adaptive attributes in durum wheat breeding programs in the Middle East and North Africa. The reference varieties are preferred by the pasta industry for their quality and therefore widely grown in Australia. The NAM population was genotyped using Diversity Arrays Technology genotyping-by-sequencing single nucleotide polymorphism (SNP) markers (Alahmad *et al.*, 2019). Allele coding used 0, 1, and 2, where 0 is the reference allele homozygote, 1 is the SNP allele homozygote and 2 is the heterozygote.

Field trials

A subset of the durum wheat NAM population and a selection of Australian durum wheat varieties were evaluated in four rainfed field trials conducted in Australia between 2017 and 2020 (Table 1), namely "2017_RW" at Roseworthy (34.30 °S; 138.41 °E), South Australia; "2019_TS" at Tosari, near Tummaville (27.51 °S; 151.27 °E), Queensland; and "2017_WW" and "2020_WW" at Warwick (28.12 °S; 152.06 °E), Queensland. The trials adopted partially replicated row-column designs (Cullis *et al.*, 2006), with the exception of 2017_RW which used a randomized complete block design with three replicates. The total number of genotypes ranged from 147 to 309 across the trials, with pairs of trials having between 51 and 146 genotypes in common. For all trials, starting fertilizer was applied at sowing so that nutrients were not limited, and weeds and insects were controlled as required. Based on the nearest

weather station to each trial site, weather information was acquired from the Bureau of Meteorology (http://www.bom.gov.au/) and the SILO database (Jeffrey *et al.*, 2001).

To monitor soil moisture and estimate the impact of drought stress on yield in the 2020_WW trial, two check genotypes (DBA Aurora and Fadda98) were sown in dryland and irrigated blocks next to the main experiment. Both blocks were sown on the same day as the main trial. The rainfed block was adjacent to 2020_WW and the irrigation block was adjacent to the rainfed block (separated by buffer rows to prevent lateral movement of soil moisture across treatments). Plot size was consistent with the main trial and each treatment was sown in a completely randomized block design, using 12 replicates in the dryland treatment and 6 replicates in the irrigation treatment. About 20 mm of water was applied through drip tape irrigation every 1-2 weeks to ensure a stress-free growing environment. To determine soil water availability, soil water content was measured for both dryland and irrigated blocks at one week pre-anthesis and at anthesis. In each strip, two soil cores were collected from DBA Aurora and Fadda98 plots in both treatments. Each core was divided into 20cm soil layers: 0–20, 20–40, 40–60, 60–80, 80–100, and 100–120 cm. A subsample from each soil layer was immediately weighed to obtain fresh weight, and then dried to a constant weight at 105 °C. Soil water content for each layer was calculated as [(fresh weight-dry weight)/dry weight]×100%.

Data collection

The 2020_WW trial was subjected to intensive canopy phenotyping and resulting phenotypes were used for association mapping. The trial comprised 309 genotypes evaluated using a p-rep design (~38%) of 456 plots (6 m × 1.05 m, 4 rows) (Table 2). NDVI data was captured for each plot every 1-2 weeks, specifically 22, 29, 36, 43, 50, 63, 70, 78, 85, 91, 99 and 106 days after sowing (DAS) using a GreenSeeker^{TM} handheld sensor (NTech Industries, Ukiah, CA, USA). Measurements were recorded on sunny and still days, by holding the sensor at approximately 0.6 m height above the crop canopy of the central two rows while walking through the crop at a constant rate. Canopy cover images were also captured for all plots using a mobile phone camera (Apple iPhone10), at 29, 36, 43 and 50 DAS. The RGB images were processed using Canopeo in the Matlab environment, for calculating fractional green canopy cover (FGCC) that measures the canopy surface area (Patrignani and Ochsner, 2015). In each plot, the number of spikes was manually recorded for an inner row (1 m length) to determine spike number per unit area (SN) and spike length (SL) was recorded for six plants. Plant height (PH) of three random plants in each plot was measured at maturity from ground to the top of the spike, excluding the

awn length. Flowering time (DTF) was recorded as DAS to 50% flowering (Zadok's growth stage 65) of all plants in a plot (Zadoks *et al.*, 1974). The crop was harvested using a small-plot machine harvester to obtain yield data.

To investigate the relationship between NDVI and crop developmental stages in the 2020_WW trial, a small panel of lines were selected for growth stage tracking from sowing to flag leaf emergence. The panel comprised 11 genotypes, which were selected based on divergent yield performance in previous rainfed yield trials (i.e., high yielding and low yielding lines). Each genotype was replicated 2-3 times in the trial (total 23 plots). Each plot was monitored for Zadoks' growth stages (GS) and 10 plants in the middle two rows of each plot were tagged for tracking tiller number until flag leaf emergence at 16, 22, 29, 36, 43, 50, 57, 63, 70, 78, and 85 DAS.

To investigate yield effects of SNPs associated with canopy development, analyses used yield data from the 2020_WW trial, plus data from the three other yield (2017_WW, 2017_RW and 2019_TS; Table 1). DTF was captured in all trials, except for 2017_RW (Table 1).

Analysis of phenotypic data

Spatial analyses were conducted for each trait to correct for spatial heterogeneity within each trial. A linear mixed model was fitted in ASReml-R to estimate adjusted genotype means (best linear unbiased estimates; BLUEs) for all traits in each trial as follows (Butler *et al.*, 2009):

$$y_{ijkm} = \mu + Rep_m + R_j + C_k + G_{i(m)} + e_{ijk(m)} \quad (1)$$

where y_{ijkm} denotes the plot observation of genotype *i* in replicate *m*, row *j* and column *k*, was modelled by fitting fixed effects for the overall mean (μ) and genotype *i* ($G_{i(m)}$); and random effects for replicate *m* (Rep_m), row *j* (R_j) and column *k* (C_k); and $e_{ijk(m)}$ represents the vector of spatially correlated residuals. The variance components of R_j, C_k and $e_{ijk(m)}$ were assumed to follow $R_j \sim N(0, \sigma_r^2)$, $C_k \sim N(0, \sigma_c^2)$ and $e_{ijk(m)} \sim N(0, \text{AR1} \otimes \text{AR1}\ \sigma^2)$, respectively. To correct for known or expected sources of variation that were suspected to have some effects on traits, the model was tested to assess the need for fitting of covariates (i.e., differences in establishment between genotypes, lodging). The covariates and random terms were evaluated with Wald chi-squared test and likelihood ratio test, respectively. The model was adjusted according to the identified significant terms at $\alpha = 0.05$. Except for the replicate, non-significant

model terms were dropped in an attempt to obtain the best fit. Slight modifications were made for analysing 2017_RW, where the residual term was modelled by a two-dimensional spatial model with correlation in row direction only.

Time-series modelling of canopy development used NDVI recorded from sowing to the peak of NDVI measures at 78 DAS (Fig. 1). To describe the trend of longitudinal BLUEs for NDVI, a smoothing spline was implemented in ASreml-R (Verbyla *et al.*, 1999). To summarize the NDVI growth curve, AUC was calculated using the following formula:

$$\text{AUC} = \sum_{i=1}^{n} \left[\frac{NDVI_{(i+1)} + NDVI_i}{2}\right] \left[T_{(i+1)} - T_i\right] \quad (2)$$

Where $NDVI_i$ is the NDVI prediction at the ith DAS; T_i is the i^{th} DAS; and n is the number of DAS of interest after i.

Association mapping

All data captured at the 2020_WW trial were used to perform association mapping. Genotype data was subjected to quality control, which excluded genotypes with > 20% missing marker information and markers with a call rate < 90% and a minor allele frequency (MAF) < 5%.

Two different approaches were used to map QTL for canopy development. The first approach used BLUEs for NDVI at each time-point. The second approach used the AUC based on spline modelling of time series NDVI. Population structure was investigated using principal component analysis (PCA). An appropriate number of principal components (PCs) were determined by estimating the variances of PC scores. The retained PCs were included as covariates in association tests carried out with "FarmCPU" in R (Liu *et al.*, 2016). The *p*-values of marker–trait associations (MTA) were adjusted in a multiple comparison procedure using false discovery rate (FDR) (Benjamini and Hochberg, 1995). Only associations with adjusted *p*-values (p-$_{\text{FDR}}$) less than 0.05 were considered as statistically significant and reported. For each QTL, the positive allele was determined as the allele associated with an increase in trait value. Data from each homozygous allele were tested for normality and homogeneity of variance. The means of genotypes carrying different homozygous alleles were statistically compared by independent t-tests. In several cases where data did not meet the normality criteria, non-parametric Wilcoxon rank sum test was performed to compare the allelic effect on traits.

Marker × environment analysis

The marker × environment interaction (M × E) was analysed with a linear mixed model, in a multi-environment context using all four field trials (Table 1):

$$y = \mu + E + M + M \times E + G + G \times L + G \times Y + e \quad (3)$$

where y is the vector of yield BLUEs; μ is the general mean; E represents trial; M denotes SNP; $M \times E$ is the interaction term between SNP and trial; G is genotype; $G \times L$ is the genotype by location interaction; $G \times Y$ is the genotype by year interaction, and e is the residual, assumed independent with identical distribution. In the model, E, M, and $M \times E$ were fixed effects, whereas G, $G \times L$ and $G \times Y$ were treated as random effects.

The SNP effect was modelled as the sum of a main effect common to all tested environments (M), plus the interaction term representing environments-specific deviations (M × E). Since M × E was tested conditional on the main effect, no attempt was made to interpret the SNP main effect when M × E is significant (Malosetti *et al.*, 2013). When M × E is not significant, the SNP main effect could be sufficient to represent the SNP effect. After testing, only SNPs with either significant main effect or M × E effects were reported and further investigated. The predicted means of each SNP allele × trial combination were compared with Tukey's HSD test.

A summary of the key steps and workflow involved from modelling NDVI time series data to the M × E analysis is provided in Fig. 2.

Results

Field environments experienced variable rainfall patterns

The amount of in-crop rainfall varied across the four trials, ranging from 12.8 mm (2019_TS) to 320.7 mm (2017_RW). While 2019_TS received the least in-crop rainfall (only 12.8 mm) the trial was sown into a full soil profile and the soil is described as deep with high water-holding capacity. This delayed water stress until the grain filling period and the site recorded the lowest mean yield (2.24 tonnes ha^{-1}) in comparison with other trials (Fig. S4C, Table 1). The distribution of rainfall through the season also varied across the trials (Fig. S4). For example, 2017_RW experienced a typical Mediterranean-type environment, where most rainfall occurred early in the season. In contrast, the two trials conducted at Warwick received

more rainfall during the critical grain filling period (Fig. S4B, D). The highest average yield was obtained in 2017_WW, which was on average 1 tonne ha^{-1} higher than 2017_RW and 2020_WW, and 2.7 tonnes ha^{-1} higher than 2019_TS (Table 1).

To quantify the degree of water stress in the 2020_WW canopy phenotyping trial, soil cores were sampled from dryland and irrigated strips adjacent to the main trial. Sampling performed one week prior to anthesis revealed significant differences in soil moisture (all soil depths from 0 - 1.2 m) for the dryland treatment compared to the irrigated treatment (Fig. S7A). At anthesis, soil moisture was further depleted, particularly at depth (Fig. S7A). DBA Aurora and Fadda98 obtained significantly higher yield in the irrigated treatment (Fig. S7B). Based on average yield differences between dryland and irrigated treatments, the degree of water stress experienced in the 2020_WW trial resulted in an approximate average yield loss of 1.1 tonnes ha^{-1}.

Relationships between NDVI, phenology traits and yield-related traits

The 309 NAM genotypes evaluated in 2020_WW trial displayed a high degree of phenotypic variation for temporal NDVI (Fig. 1). Phenotypic variation in NDVI was largest at the beginning of the growing season, reached a peak at 36 DAS and reduced thereafter. The NDVI reached an average peak value of 0.9 at 78 DAS (Table 3). The Pearson correlation among all traits was computed (Fig. 3). For a specific time-point NDVI, its correlations with other timepoints decreased with increasing developmental stage. Positive correlations between NDVI and SL were significant at 29 and 78 DAS ($p < 0.05$). A reverse trend was observed for SN, where NDVI in the early season (22 and 29 DAS) was negatively correlated with SN. For plant height, the only correlation with NDVI was evident at 50 DAS ($p < 0.05$). Further, NDVI captured over time was negatively correlated with DTF (Fig. 3), with higher NDVI associated with faster time to flowering. No direct NDVI-yield relationship was found before 63 DAS in our study. Rather, NDVI recorded closer to flowering time was more highly related to final yield, as the strongest correlation between NDVI and yield was observed at 78 DAS ($p < 0.001$).

Modelling NDVI over time to estimate growth stages

The longitudinal data fitted with a spline showed that the NDVI growth curves overall, increased slowly initially, then rapidly, before reaching a final plateau (Fig. 4). This suggested three different growth phases likely involved in canopy development in durum wheat. Although the trends of these curves were more or less in parallel over time, the distribution of genotype-specific NDVI trajectories indicated some heterogeneity in each phase, leading to variation in

phase-specific AUC traits. For this reason, the entire simulated AUC during the vegetative stage (AUC_VS) could be divided into three phases, each illustrating a different growth status, to capture phase-specific variation that contributes to the overall canopy development.

To understand how NDVI dynamics reflected changes in vegetation phenology, 11 genotypes including 10 NAM lines and the reference variety DBA Aurora were investigated. Given the similar phenology of the 11 genotypes, Zadok's GS20 (start of tillering) and GS31 (first node) were aligned with 29 and 63 DAS (Fig. S1), respectively. Since no significant change was observed for the tiller number of most genotypes from 57-63 DAS (Fig. S1), Zadok's GS30 (start of stem elongation) was estimated at 60 DAS. To evaluate the use of NDVI to define the growth stage, we hereafter used 30 and 60 DAS as two breakpoints to approximate GS20 and GS30, respectively.

Using 30 DAS as the first breakpoint, the NDVI trajectories of genotypes displayed two distinct growth patterns before and after the point. For instance, the sharp increase in NDVI after 30 DAS suggested a transition from seedling to tillering stage. According to the fitted NDVI curves, most genotypes reached the start of maximum canopy cover at approximately 60 DAS (Fig. 4). This finding aligned with the start of the maximum canopy cover as indicated by time-point NDVI measures (Fig. 1), where NDVI after 63 DAS remained constant. As such, the estimated transition from tillering to stem elongation by the NDVI curve was deemed reasonably accurate. However, to further identify and interpret phenology metrics, the saturation issue may impact NDVI-based recommendations as NDVI becomes insensitive to changes in canopy structure when the crop reaches canopy closure.

The relationship between time-point NDVI and AUC traits

NDVI curves were binned into three growth stages: seedlin*g* stage (SS, 0-30 DAS), tillering stage (TL, 30-60 DAS) and stem elongation stage (SE, 60-78 DAS) (Fig. 4). Accordingly, the AUC traits for each stage were designated AUC_SS, AUC_TL and AUC_SE, and were used to quantify the cumulative status for each stage. Given this, the same duration of each growth stage was applied to all studied genotypes. Hence, differences in growth rate appeared to contribute to variation in AUC, where higher AUC values represented faster canopy development and closure.

As expected, because of the linear nature of the operations involved, stage-specific AUC traits showed strong correlations with NDVI measured within the respective stage (Fig. 3). Moreover, stage-specific AUC traits were also found to correlate well with NDVI measured at other stages. The integral NDVI approach ensured that canopy differences related to yield formation were captured. For example, AUC_SE was correlated with yield, but only some of the NDVI time-points during SE showed significant correlations with yield (e.g., 70 DAS was not correlated, but readings captured at 63 DAS and 78 DAS were, as shown in Fig. 3). These results highlighted the robustness and suitability of the approach for proceeding with genetic dissection studies.

Time-point NDVI and AUC correlate with canopy cover

NDVI displayed a positive linear relationship with FGCC before NDVI reached the maximum value of 0.9 (Fig. 5). Most genotypes obtained 80% FGCC at 50 DAS. Thus, rapid growth during the tillering stage could almost achieve canopy closure before the start of stem elongation. Moreover, all AUC traits showed significant correlations with FGCC, except for AUC_SS (Fig. 3). This highlights the value of NDVI to estimate canopy cover as measures were similar to RGB-based estimates. As such, a higher NDVI and/or a greater AUC value represented a larger canopy that was faster to close.

Association mapping for canopy development

A total of 5,298 high-quality polymorphic SNP markers for 309 lines were used for association mapping. The PCA revealed six clusters in the NAM population (Fig. S2A), which aligned with the family structure (Table 2). The first five PCs were used as covariates in association mapping, because explained variance rapidly decreased until PC = 5 and changed little thereafter (Fig. S2B). The first two PCs explained ~ 23% of the genetic variance (Fig. S2B).

Association mapping was performed for time-point NDVI, stage-based AUC, crop phenology-related traits, spike traits and grain yield traits captured in the 2020_WW trial. Using time-point NDVI, a total of 11 significant MTAs were detected across nine chromosomes, including 2A, 2B, 3A, 4A, 4B, 5A, 6A, 6B and 7A (Table 4). Among these, only one SNP was detected for more than one NDVI time-point (i.e., SNP 1271404 on chromosome 2A). Notably, in agreement with the genetic variation in NDVI (Fig. 1), most MTAs were identified at specific time-points between 29 and 50 DAS.

To identify markers associated with AUC, we conducted association mapping using the following traits: AUC_SS, AUC_TL, AUC_SE and AUC_VS. This detected six significant MTAs, of which five were associated with more than one AUC trait. SNP 1271404 on chromosome 2A, was also detected using time-point NDVI measures during the TL growth stage. Mapping AUC enabled the identification of five additional signals, on chromosome 2A (SNP 4004899), 2B (SNPs 1095539 and 1108975), 4A (SNP 3946360) and 5B (SNP 1093322) (Table 4).

Interestingly, most MTAs for phenology-related traits were independent of MTAs associated with canopy development, except for SNP 2256343 on chromosome 2A which was associated with NDVI_50DAS and DTF (Table 4).

M × E analysis revealed markers associated with grain yield

The M × E interaction analysis was conducted to assess the significance and strength of the SNP effects on yield across trials. Analyses focussed on 13 SNPs that were associated with canopy development and segregating in population subsets evaluated across all trials.

The allelic effects on canopy development were first explored using data collected from 2020_WW. For all SNPs, the allele associated with either higher NDVI or larger AUC was defined as the positive allele, which was linked to rapid canopy closure (Table 4). To account for the fact that SNP 2256343 was also associated with flowering time (Fig. S3, Table 4), we excluded the top 20% and bottom 20% of genotypes in 2019_TS and 2020_WW based on DTF. As a result, 131 and 185 genotypes that showed no significant difference in DTF were retained in 2019_TS and 2020_WW, respectively, and were used for the analysis of yield effects associated with SNP 2256343.

A linear mixed model approach was employed to evaluate effects for each of the 13 SNPs using yield data from four rainfed trials (Table 1). In the current study, no significant marker main effect was detected for yield. Instead, 9 markers showed significant M × E interactions for yield (Table 5). Notably, SNP 1095539, 3949783, 4404447 and 5324123 showed significant yield effects in 2017_WW, 2017_WW, 2017_RW, and 2020_WW, respectively (Table 5). Alleles associated with a significant yield benefit were associated with slow canopy closure (Fig. S5; Table 4, 5). Therefore, these four SNPs of interest were subjected to further investigation.

Alleles influencing canopy development and yield were also associated with spike length and spike number

Three of the four marker alleles associated with a slower closing canopy and yield (1095539, 3949783, 4404447 and 5324123) also showed associations with SL or SN. Interestingly, SNP 5324123 was strongly associated with both SL and SN in 2020_WW, but the yield benefit in this trial was related to a reduction in SN (Fig. S6D, Table 5-6). Similarly, the significant yield effect of SNP 1095539 in 2017_WW was associated with SL (Fig. S6D, Tables 5-6). On the other hand, SNP 3949783 was associated with SL in 2020_WW but not yield (Tables 5-6). SNP 4404447 was not associated with either component traits (Table 6). Notably, SNP 4404447 was not associated with yield in 2017_WW and 2020_WW and these were the environments where data for SL and SN were captured (Table 5). Overall, alleles associated with slow canopy closure supported yield, however, the contribution and yield benefit associated with pleiotropic effects on SL and SN appeared highly context dependent across the environments.

Discussion

Wheat yield is determined by the interaction between source, which is the availability of photoassimilates, and sink, which is the number of grains per unit area (Reynolds *et al.*, 2017). Canopy development underpins yield potential, as it influences the capture of light, water use, transpiration, and overall biomass production. In water-limited environments, optimal canopy development balances water use both pre- and post-anthesis to maximise yield. For example, while slow canopy development may not favour biomass accumulation pre-anthesis, it can help to conserve soil moisture for the critical grain filling period. However, in environments where water is non-limiting, optimal canopy development should maximise biomass production and overall sink strength as there is no penalty of high water-use early in the season. This study revealed a high degree of variation for temporal canopy dynamics in elite durum wheat populations derived from Australian × ICARDA crosses, which could be used to improve durum wheat adaptation to a range of target environments. New knowledge of the underlying genetics and value of canopy developmental traits described in this study provide important steps towards the development of new cultivars with improved resource-use efficiency to maximise crop yield.

Using NDVI to measure canopy development

NDVI serves as an easy-to-measure indicator of canopy development in real time. The link between NDVI and canopy development is strongly underpinned by the functional relationship between NDVI and aboveground biomass. In accordance with previous research, time-specific NDVI measures during the early growing period were generally poor predictors of yield (Magney *et al.*, 2016), whereas NDVI captured at the peak of canopy development is more associated with yield. This is somewhat expected due to the complexity underpinning yield development. Furthermore, the stem elongation to flowering phase is considered the most critical for determining grain number and ultimately sink strength.

Phenological and environmental changes over time affect the canopy status represented by NDVI. Therefore, the use of the NDVI integral (i.e., area under the curve) provides an advantage over time specific NDVI as it captures the impact of those changes on canopy development. To accurately assess long-term patterns of canopy development, regular NDVI measurements are required. Nonlinear models have been widely used to account for the complexities of plant growth (Paine *et al.*, 2012; Villegas *et al.*, 2001). Previous studies comparing different models to characterise the dynamics of NDVI over time found that spline-fitting better approximated the variation of smoothed NDVI values than other non-linear functions and was more suitable for describing the time-series model (Sun *et al.*, 2017; Vorobiova and Chernov, 2017). In this study, the trajectories of smoothed NDVI data showed a typical temporal pattern of NDVI evolution during the vegetative stage, where crop emergence was followed by a rapid growth period, then a relatively stable period of maximum vegetation approaching anthesis. Therefore, cumulative NDVI at specific growth stages could be used to gain insights of the physiological drivers underpinning grain yield.

The genetics of canopy development

To identify loci underpinning canopy development, time-point NDVI data were treated as independent traits and association mapping was performed for each timepoint to identify time-specific NDVI (Fig. 2). Next, spline-fitted curve-derived AUC was subject to mapping, and results were compared to mapping of time-point NDVI.

Time-point NDVI measures were highly correlated, suggesting the underlying genetic controls either provide long-term regulation of canopy growth or have prolonged effects originating from an early growth phase. This was further confirmed in the mapping results, where the 2A QTL (SNP 1271404) was detected by multiple time-point NDVI.

AUC in the current study was used to capture the genetic basis of canopy growth with respect to key developmental stages. However, some QTL could only be detected using time-point NDVI and it is unclear why these QTL could not be captured using the AUC approach. One possible explanation is that they were transient QTL sensitive to time of data collection, whereas AUC represented a period of growth, and therefore more likely detected loci with more consistent and robust effects. Thus, time-point NDVI and AUC had different mapping strengths and were complementary to each other. The use of AUC for mapping time-dependent canopy development should be implemented on a case-by-case basis, with the aim of ensuring good quality data for use in modelling canopy dynamics. Additionally, AUC values should not be directly compared across different studies, as AUC is a product of many contributing factors, including the environment, modelling approach, phenotyping method and crop phenology.

This study uncovered four SNPs on chromosomes 2B (1095539 and 3949783), 4A (5324123) and 6A (4404447) that could be useful for durum wheat breeding, as alleles associated with slow canopy closure were linked to a yield advantage in some environments, but not a yield penalty in other environments. Notably, all four SNPs were not associated with DTF, which improves the utility of the genes from a breeding perspective, as canopy development could be manipulated without shifting flowering time. Three of the four SNPs (1095539, 3949783 and 5324123) were also associated with yield component traits: SN and SL, where SL is considered a proxy for the number of grains per spike (Baye *et al.*, 2020). Interestingly, most of these SNPs were detected using NDVI measures recorded at the early tillering stage, an important phase for spike formation in wheat (Khadka *et al.*, 2020), when no correlation between NDVI and yield was found. The 2B (3949783) and 6A (4404447) regions have previously been reported to influence a range of spike traits including spike dry matter, grain weight per spike, grains per spike and grain weight (Giunta *et al.*, 2018; Mangini *et al.*, 2018; Patil *et al.*, 2013; Peleg *et al.*, 2009; Soriano *et al.*, 2017). While the 4A region (5324123) has not previously been reported for SN and SL per se, it has been reported to influence similar or related traits, including biomass, harvest index, spike harvest index, spike density (spikelet number/SL), and importantly grain yield (Mengistu *et al.*, 2016; Peleg *et al.*, 2011; Peleg *et al.*, 2009; Tzarfati *et al.*, 2014).

Yield benefits of slow canopy development, trade-offs and pleiotropic effects

Four QTL for slow canopy development were associated with yield in three of the four rainfed environments (2017_RW, 2017_WW and 2020_WW). These three trials likely experienced

water stress at anthesis, whereas 2019_TS received very little in-crop rainfall (Fig. S4C) and likely experienced pre-anthesis water stress. This highlights the value of slow canopy development in water-limited environments that experience drought at anthesis or during the grain filling period. As discussed above, the benefit of a slow closing canopy likely manifests from water savings that support yield formation during grain filling. Without having sufficient environmental data to perform robust envirotyping in APSIM (Chenu *et al.*, 2013), it is difficult to quantify the degree of water-stress in the rainfed experiments. However, soil moisture was measured in the dryland and irrigated strips adjacent to the 2020_WW trial. Soil moisture under the rainfed conditions was clearly depleted at anthesis, particularly in deeper soil layers (Fig. S7A), and the water limitation resulted in an average yield loss of 1.1 tonnes ha^{-1}. This highlights the impact of drought under rainfed conditions in Australia, despite three of the four trials being conducted on deep soils with a high water-holding capacity. Although soil moisture data was not available for 2017_WW, the same site was used for 2020_WW. In 2017_WW the trial received less in-crop rainfall compared to 2020_WW (Table 1), suggesting it likely experienced similar or more severe water stress than 2020_WW. Terminal drought often occurs in Mediterranean-type environments, such as South Australia. In 2017_RW, about 90% of the in-crop rainfall occurred from May to September, suggesting the trial experienced water stress late in the season (Fig. S4A). Regardless of the delayed onset of water stress (compared with the Warwick sites in Queensland), the four QTL associated with slow canopy development contributed positive yield effects.

Harvested wheat yield is a result of three components: spike number per unit area, grain number per spike, and average grain weight (Simmonds *et al.*, 2014; Zhang *et al.*, 2018). In the current study, the relationship between SL, SN and yield varied across the two trials (2017_WW and 2020_WW). Specifically, SL showed a significant correlation with yield in 2017_WW, but not in 2020_WW (Fig. S6A, C), while SN showed a significant correlation with yield in 2020_WW, but not in 2017_WW (Fig. S6B, D). Previous studies in both bread and durum wheat have reported positive relationships between SL and yield under water-limited conditions (Munir *et al.*, 2007; Nofouzi, 2018). In this scenario, genotypes with fewer tillers could accumulate less biomass, but produce longer spikes with more grains, to achieve a yield advantage.

It is plausible that loci associated with canopy development and yield component traits could be involved in modulating root architecture. The study by Voss-Fels *et al.* (2018) reported that allelic variation at *Vrn1*, a key gene in the wheat flowering pathway, not only influences spike

and canopy development, but also root system architecture. In the current study, a QTL on 2B (1095539) associated with AUC_SS and AUC_SE was positioned in close proximity with previously reported QTL for root growth angle and primary root length (Maccaferri *et al.*, 2016). Thus, either closely positioned or pleiotropic loci on chromosome 2B could be important for both above- and below-ground developmental traits.

Clearly, the value of different yield component traits in durum wheat is highly context dependent, and genotypes can exploit a range of pathways to maximise yield in each environment. A priority for future research is to understand the complex interactions and possible pleiotropic effects of loci influencing both canopy development and yield component traits. Such insight will enable selection and deployment of desirable gene combinations in breeding programs seeking to develop new varieties with improved resilience and productivity.

Acknowledgements

Funding was supported by Grain Research and Development Corporation (GRDC; project code UOQ1903-007RTX).

Author Contribution

YCK, LTH and SA conceived and designed the study. SUK and SA contributed to developing the plant materials. YCK, SA, JA and LTH performed the phenotyping. SV processed RGB images using Canopeo. YCK analysed the data. YCK and SVH prepared the figures. DBK and KPV advised on the data analysis. KC and JC advised on interpretation of trait relationships. YCK wrote the manuscript. AKB contributed to physiological understanding of the data, DBK, AKB, MRS and LTH edited the manuscript. All authors read and reviewed the manuscript.

Data Availability Statement

All data supporting the findings of this study are available within the paper and within its supplementary materials published online.

References

Alahmad S, El Hassouni K, Bassi FM, Dinglasan E, Youssef C, Quarry G, Aksoy A, Mazzucotelli E, Juhasz A, Able JA, Christopher J, Voss-Fels KP, Hickey LT. 2019. A major root architecture QTL responding to water limitation in durum wheat. Frontiers in Plant Science 10.

Bassi FM, Nachit MM. 2019. Genetic gain for yield and allelic diversity over 35 years of durum wheat breeding at ICARDA. Crop Breed. Genet. Genom 1, 1-19.

Baye A, Berihun B, Bantayehu M, Derebe B. 2020. Genotypic and phenotypic correlation and path coefficient analysis for yield and yield-related traits in advanced bread wheat (Triticum aestivum L.) lines. Cogent Food & Agriculture 6.

Benjamini Y, Hochberg Y. 1995. Controlling the False Discovery Rate: A Practical and Powerful Approach to Multiple Testing. Journal of the Royal Statistical Society Series B-Statistical Methodology 57, 289-300.

Borrell AK, Mullet JE, George-Jaeggli B, van Oosterom EJ, Hammer GL, Klein PE, Jordan DR. 2014. Drought adaptation of stay-green sorghum is associated with canopy development, leaf anatomy, root growth, and water uptake. Journal of Experimental Botany 65, 6251-6263.

Brown ME, de Beurs KM. 2008. Evaluation of multi-sensor semi-arid crop season parameters based on NDVI and rainfall. Remote Sensing of Environment 112, 2261-2271.

Bustos-Korts D, Boer MP, Malosetti M, Chapman S, Chenu K, Zheng BY, van Eeuwijk F. 2019. Combining Crop Growth Modeling and Statistical Genetic Modeling to Evaluate Phenotyping Strategies. Frontiers in Plant Science 10.

Butler DG, Cullis BR, Gilmour AR, Gogel BJ. 2009. ASReml-R reference manual. The State of Queensland, Department of Primary Industries and Fisheries, Brisbane.

Cabrera-Bosquet L, Molero G, Stellacci AM, Bort J, Nogues S, Araus JL. 2011. NDVI as a potential tool for predicting biomass, plant nitrogen content and growth in wheat genotypes subjected to different water and nitrogen conditions. Cereal Research Communications 39, 147-159.

Carlson TN, Ripley DA. 1997. On the relation between NDVI, fractional vegetation cover, and leaf area index. Remote Sensing of Environment 62, 241-252.

Chenu K, Deihimfard R, Chapman SC. 2013. Large-scale characterization of drought pattern: a continent-wide modelling approach applied to the Australian wheatbelt spatial and temporal trends. New Phytologist 198, 801-820.

Christopher JT, Christopher MJ, Borrell AK, Fletcher S, Chenu K. 2016. Stay-green traits to improve wheat adaptation in well-watered and water-limited environments. Journal of Experimental Botany 67, 5159-5172.

Christopher JT, Veyradier M, Borrell AK, Harvey G, Fletcher S, Chenu K. 2014. Phenotyping novel stay-green traits to capture genetic variation in senescence dynamics. Functional Plant Biology 41, 1035-1048.

Collins B, Chapman S, Hammer G, Chenu K. 2021. Limiting transpiration rate in high evaporative demand conditions to improve Australian wheat productivity. in silico Plants 3, diab006.

Condorelli GE, Maccaferri M, Newcomb M, Andrade-Sanchez P, White JW, French AN, Sciara G, Ward R, Tuberosa R. 2018. Comparative aerial and ground based high throughput phenotyping for the genetic dissection of NDVI as a proxy for drought adaptive traits in durum wheat. Frontiers in Plant Science 9.

Cullis BR, Smith AB, Coombes NE. 2006. On the design of early generation variety trials with correlated data. Journal of Agricultural Biological and Environmental Statistics 11, 381-393.

De Vita P, Nicosia OL, Nigro F, Platani C, Riefolo C, Di Fonzo N, Cattivelli L. 2007. Breeding progress in morpho-physiological, agronomical and qualitative traits of durum wheat cultivars released in Italy during the 20th century. European Journal of Agronomy 26, 39-53.

Gamon JA, Field CB, Goulden ML, Griffin KL, Hartley AE, Joel G, Peñuelas J, Valentini R. 1995. Relationships between NDVI, canopy structure, and photosynthesis in three Californian vegetation types. Ecological Applications 5, 28-41.

George-Jaeggli B, Mortlock MY, Borrell AK. 2017. Bigger is not always better: Reducing leaf area helps stay-green sorghum use soil water more slowly. Environmental and Experimental Botany 138, 119-129.

Gevrek MN, Atasoy GD. 2012. Effect of post anthesis drought on certain agronomical characteristics of wheat under two different nitrogen application conditions. Turkish Journal of Field Crops 17, 19-23.

Giunta F, De Vita P, Mastrangelo AM, Sanna G, Motzo R. 2018. Environmental and Genetic Variation for Yield-Related Traits of Durum Wheat as Affected by Development. Frontiers in Plant Science 9.

Goodwin AW, Lindsey LE, Harrison SK, Paul PA. 2018. Estimating Wheat Yield with Normalized Difference Vegetation Index and Fractional Green Canopy Cover. Crop Forage & Turfgrass Management 4.

Hammer GL, McLean G, van Oosterom E, Chapman S, Zheng BY, Wu A, Doherty A, Jordan D. 2020. Designing crops for adaptation to the drought and high-temperature risks anticipated in future climates. Crop Science 60, 605-621.

Jeffrey SJ, Carter JO, Moodie KB, Beswick AR. 2001. Using spatial interpolation to construct a comprehensive archive of Australian climate data. Environmental Modelling & Software 16, 309-330.

Khadka K, Earl HJ, Raizada MN, Navabi A. 2020. A Physio-Morphological Trait-Based Approach for Breeding Drought Tolerant Wheat. Frontiers in Plant Science 11.

Kwak IY, Moore CR, Spalding EP, Broman KW. 2016. Mapping uantitative trait loci underlying function-valued traits using functional principal component analysis and multi-trait mapping. G3-Genes Genomes Genetics 6, 79-86.

Liu XL, Huang M, Fan B, Buckler ES, Zhang ZW. 2016. Iterative Usage of Fixed and Random Effect Models for Powerful and Efficient Genome-Wide Association Studies. Plos Genetics 12.

Lopes MS, Reynolds MP. 2012. Stay-green in spring wheat can be determined by spectral reflectance measurements (normalized difference vegetation index) independently from phenology. Journal of Experimental Botany 63, 3789-3798.

Lopez-Castaneda C, Richards RA, Farquhar GD. 1995. Variation in early vigor between wheat and barley. Crop Science 35, 472-479.

Loss SP, Siddique KHM. 1994. Morphological and physiological traits associated with wheat yield increases in Mediterranean environments. Advances in Agronomy, Vol 52 52, 229-276.

Lyra DH, Virlet N, Sadeghi-Tehran P, Hassall KL, Wingen LU, Orford S, Griffiths S, Hawkesford MJ, Slavov GT. 2020. Functional QTL mapping and genomic prediction of canopy height in wheat measured using a robotic field phenotyping platform. Journal of Experimental Botany 71, 1885-1898.

Maccaferri M, El-Feki W, Nazemi G, Salvi S, Cane MA, Colalongo MC, Stefanelli S, Tuberosa R. 2016. Prioritizing quantitative trait loci for root system architecture in tetraploid wheat. Journal of Experimental Botany 67, 1161-1178.

Maccaferri M, Sanguineti MC, Corneti S, Ortega JLA, Ben Salem M, Bort J, DeAmbrogio E, del Moral LFG, Demontis A, El-Ahmed A, Maalouf F, Machlab H, Martos V, Moragues M, Motawaj J, Nachit M, Nserallah N, Ouabbou H, Royo C, Slama A, Tuberosa R. 2008. Quantitative trait loci for grain yield and adaptation of durum wheat (Triticum durum Desf.) across a wide range of water availability. Genetics 178, 489-511.

Magney TS, Eitel JUH, Huggins DR, Vierling LA. 2016. Proximal NDVI derived phenology improves in-season predictions of wheat quantity and quality. Agricultural and Forest Meteorology 217, 46-60.

Malosetti M, Ribaut JM, van Eeuwijk FA. 2013. The statistical analysis of multi-environment data: modeling genotype-by-environment interaction and its genetic basis. Frontiers in Physiology 4.

629 Mangini G, Gadaleta A, Colasuonno P, Marcotuli I, Signorile AM, Simeone R, De Vita P,
630 Mastrangelo AM, Laido G, Pecchioni N, Blanco A. 2018. Genetic dissection of the
631 relationships between grain yield components by genome-wide association mapping in a
632 collection of tetraploid wheats. Plos One 13.
633 Masialeti I, Egbert S, Wardlow BD. 2010. A Comparative Analysis of Phenological Curves for
634 Major Crops in Kansas. Giscience & Remote Sensing 47, 241-259.
635 Matesanz S, Ramos-Munoz M, Moncalvillo B, Teso MLR, de Dionisio SLG, Romero J,
636 Iriondo JM. 2020. Plasticity to drought and ecotypic differentiation in populations of a crop
637 wild relative. Aob Plants 12.
638 Mengistu DK, Kidane YG, Catellani M, Frascaroli E, Fadda C, Pe ME, Dell'Acqua M. 2016.
639 High-density molecular characterization and association mapping in Ethiopian durum wheat
640 landraces reveals high diversity and potential for wheat breeding. Plant Biotechnology Journal
641 14, 1800-1812.
642 Miao C, Xu Y, Liu S, Schnable PS, Schnable JC. 2020. Increased power and accuracy of causal
643 locus identification in time series genome-wide association in sorghum. Plant Physiology 183,
644 1898-1909.
645 Miralles DJ, Rharrabti Y, Royo C, Villegas D, Garcıa del Moral LF. 2002. Grain setting
646 strategies of Mediterranean durum wheat cultivars released in different periods (1900–2000).
647 *Genotype-Phenotype: Narrowing the Gaps. AAB Conference,* . Cirencester, UK.
648 Motzo R, Giunta F, Pruneddu G. 2010. The response of rate and duration of grain filling to
649 long-term selection for yield in Italian durum wheats. Crop & Pasture Science 61, 162-169.
650 Mullan DJ, Reynolds MP. 2010. Quantifying genetic effects of ground cover on soil water
651 evaporation using digital imaging. Functional Plant Biology 37, 703-712.
652 Munir M, Chowdhry MA, Malik TA. 2007. Correlation studies among yield and its
653 components in bread wheat under drought conditions. International Journal of Agriculture and
654 Biology (Pakistan).
655 Muraya MM, Chu JT, Zhao YS, Junker A, Klukas C, Reif JC, Altmann T. 2017. Genetic
656 variation of growth dynamics in maize (Zea mays L.) revealed through automated non-invasive
657 phenotyping. Plant Journal 89, 366-380.
658 Nofouzi F. 2018. Evaluation of seed yield of durum wheat (Triticum durum) under drought
659 stress and determining correlation among some yield components using path coefficient
660 analysis. Cuadernos de Investigación UNED 10, 179-183.
661 Nuttall JG, O'Leary GJ, Khimashia N, Asseng S, Fitzgerald G, Norton R. 2012. 'Haying-off' in
662 wheat is predicted to increase under a future climate in south-eastern Australia. Crop & Pasture
663 Science 63, 593-605.
664 Paine CET, Marthews TR, Vogt DR, Purves D, Rees M, Hector A, Turnbull LA. 2012. How
665 to fit nonlinear plant growth models and calculate growth rates: an update for ecologists.
666 Methods in Ecology and Evolution 3, 245-256.
667 Patil RM, Tamhankar SA, Oak MD, Raut AL, Honrao BK, Rao VS, Misra SC. 2013. Mapping
668 of QTL for agronomic traits and kernel characters in durum wheat (Triticum durum Desf.).
669 Euphytica 190, 117-129.
670 Patrignani A, Ochsner TE. 2015. Canopeo: A Powerful New Tool for Measuring Fractional
671 Green Canopy Cover. Agronomy Journal 107, 2312-2320.
672 Peleg Z, Fahima T, Korol AB, Abbo S, Saranga Y. 2011. Genetic analysis of wheat
673 domestication and evolution under domestication. Journal of Experimental Botany 62, 5051-
674 5061.
675 Peleg Z, Fahima T, Krugman T, Abbo S, Yakir D, Korol AB, Saranga Y. 2009. Genomic
676 dissection of drought resistance in durum wheat x wild emmer wheat recombinant inbreed line
677 population. Plant Cell and Environment 32, 758-779.

678 Pinto RS, Lopes MS, Collins NC, Reynolds MP. 2016. Modelling and genetic dissection of
679 staygreen under heat stress. Theoretical and Applied Genetics 129, 2055-2074.
680 Regan KL, Siddique KHM, Tennant D, Abrecht DG. 1997. Grain yield and water use efficiency
681 of early maturing wheat in low rainfall Mediterranean environments. Australian Journal of
682 Agricultural Research 48, 595-603.
683 Reynolds MP, Pask AJD, Hoppitt WJE, Sonder K, Sukumaran S, Molero G, Saint Pierre C,
684 Payne T, Singh RP, Braun HJ, Gonzalez FG, Terrile, II, Barma NCD, Hakim A, He ZH, Fan
685 ZR, Novoselovic D, Maghraby M, Gad KIM, Galal EG, Hagras A, Mohamed MM, Morad
686 AFA, Kumar U, Singh GP, Naik R, Kalappanavar IK, Biradar S, Prasad SVS, Chatrath R,
687 Sharma I, Panchabhai K, Sohu VS, Mavi GS, Mishra VK, Balasubramaniam A, Jalal-Kamali
688 MR, Khodarahmi M, Dastfal M, Tabib-Ghaffari SM, Jafarby J, Nikzad AR, Moghaddam HA,
689 Ghojogh H, Mehraban A, Solis-Moya E, Camacho-Casas MA, Figueroa-Lopez P, Ireta-
690 Moreno J, Alvarado-Padilla JI, Borbon-Gracia A, Torres A, Quiche YN, Upadhyay SR, Pandey
691 D, Imtiaz M, Rehman MU, Hussain M, Ud-Din R, Qamar M, Kundi M, Mujahid MY, Ahmad
692 G, Khan AJ, Sial MA, Mustatea P, von Well E, Ncala M, de Groot S, Hussein AHA, Tahir ISA,
693 Idris AAM, Elamein HMM, Manes Y, Joshi AK. 2017. Strategic crossing of biomass and
694 harvest index-source and sink-achieves genetic gains in wheat. Euphytica 213.
695 Rodrigues J, Inze D, Nelissen H, Saibo NJM. 2019. Source-sink regulation in crops under water
696 deficit. Trends in Plant Science 24, 652-663.
697 Royo C, Abaza M, Blanco R, del Moral LFG. 2000. Triticale grain growth and morphometry
698 as affected by drought stress, late sowing and simulated drought stress. Australian Journal of
699 Plant Physiology 27, 1051-1059.
700 Sall AT, Chiari T, Legesse W, Seid-Ahmed K, Ortiz R, van Ginkel M, Bassi FM. 2019. Durum
701 wheat (Triticum durum Desf.): origin, cultivation and potential expansion in Sub-Saharan
702 Africa. Agronomy-Basel 9.
703 Shavrukov Y, Kurishbayev A, Jatayev S, Shvidchenko V, Zotova L, Koekemoer F, de Groot
704 S, Soole K, Langridge P. 2017. Early flowering as a drought escape mechanism in plants: How
705 can it aid wheat production? Frontiers in Plant Science 8, 1950.
706 Shi SK, Azam FI, Li HH, Chang XP, Li BY, Jing RL. 2017. Mapping QTL for stay-green and
707 agronomic traits in wheat under diverse water regimes. Euphytica 213.
708 Simmonds J, Scott P, Leverington-Waite M, Turner AS, Brinton J, Korzun V, Snape J, Uauy
709 C. 2014. Identification and independent validation of a stable yield and thousand grain weight
710 QTL on chromosome 6A of hexaploid wheat (Triticum aestivum L.). Bmc Plant Biology 14.
711 Smith RCG, Adams J, Stephens DJ, Hick PT. 1995. Forecasting wheat yield in a
712 Mediterranean-type environment from the NOAA satellite. Australian Journal of Agricultural
713 Research 46, 113-125.
714 Soltani A, Galeshi S. 2002. Importance of rapid canopy closure for wheat production in a
715 temperate sub-humid environment: experimentation and simulation. Field Crops Research 77,
716 17-30.
717 Soriano JM, Malosetti M, Rosello M, Sorrells ME, Royo C. 2017. Dissecting the old
718 Mediterranean durum wheat genetic architecture for phenology, biomass and yield formation
719 by association mapping and QTL meta-analysis. Plos One 12.
720 Sun J, Rutkoski JE, Poland JA, Crossa J, Jannink JL, Sorrells ME. 2017. Multitrait, Random
721 Regression, or Simple Repeatability Model in High-Throughput Phenotyping Data Improve
722 Genomic Prediction for Wheat Grain Yield. Plant Genome 10.
723 Teal RK, Tubana B, Girma K, Freeman KW, Arnall DB, Walsh O, Raun WR. 2006. In-season
724 prediction of corn grain yield potential using normalized difference vegetation index.
725 Agronomy Journal 98, 1488-1494.

726 Tzarfati R, Barak V, Krugman T, Fahima T, Abbo S, Saranga Y, Korol AB. 2014. Novel
727 quantitative trait loci underlying major domestication traits in tetraploid wheat. Molecular
728 Breeding 34, 1613-1628.
729 Verbyla AP, Cullis BR, Kenward MG, Welham SJ. 1999. The analysis of designed experiments
730 and longitudinal data by using smoothing splines. Journal of the Royal Statistical Society Series
731 C-Applied Statistics 48, 269-300.
732 Villegas D, Aparicio N, Blanco R, Royo C. 2001. Biomass accumulation and main stem
733 elongation of durum wheat grown under Mediterranean conditions. Annals of Botany 88, 617-
734 627.
735 Vorobiova N, Chernov A. 2017. Curve fitting of MODIS NDVI time series in the task of early
736 crops identification by satellite images. 3rd International Conference Information Technology
737 and Nanotechnology (Itnt-2017) 201, 184-195.
738 Voss-Fels KP, Robinson H, Mudge SR, Richard C, Newman S, Wittkop B, Stahl A, Friedt W,
739 Frisch M, Gabur I, Miller-Cooper A, Campbell BC, Kelly A, Fox G, Christopher J, Christopher
740 M, Chenu K, Franckowiak J, Mace ES, Borrell AK, Eagles H, Jordan DR, Botella JR, Hammer
741 G, Godwin ID, Trevaskis B, Snowdon RJ, Hickey LT. 2018. VERNALIZATION1 Modulates
742 Root System Architecture in Wheat and Barley. Molecular Plant 11, 226-229.
743 Xue JR, Su BF. 2017. Significant remote sensing vegetation indices: a review of developments
744 and applications. Journal of Sensors 2017.
745 Zadoks JC, Chang TT, Konzak CF. 1974. A decimal code for the growth stages of cereals.
746 Weed research 14, 415-421.
747 Zhang JL, Gizaw SA, Bossolini E, Hegarty J, Howell T, Carter AH, Akhunov E, Dubcovsky J.
748 2018. Identification and validation of QTL for grain yield and plant water status under
749 contrasting water treatments in fall-sown spring wheats. Theoretical and Applied Genetics 131,
750 1741-1759.
751

Table 1. Attributes of the four rainfed yield trials conducted between 2017 and 2020.

Trial	2017_RW	2017_WW	2019_TS	2020_WW
Location	Roseworthy	Warwick	Tosari	Warwick
SD[1]	09/05/2017	22/06/2017	08/07/2019	01/07/2020
HarvD[2]	22/11/2017	15/11/2017	15/11/2019	26/11/2020
No. of plots[3]	576	336	440	456
ICR (mm)[4]	320.7	137.5	12.8	185.0
GDD (°C)[5]	2468	2190	2222	2377
Range of DTF[6]	na[7]	96-108	84-102	90-104
Yld (t-ha^{-1})[8]	3.95	4.91	2.24	3.87
No. of geno[9]	149	147	217	309
Traits measured	Yld	SL[10], SN[11], DTF, Yld	DTF, Yld	Canopy related traits[12], SL, SN, DTF, PH[13], Yld

[1] Sowing date.
[2] Harvesting date.
[3] Total number of plots in the experiment.
[4] In-crop rainfall.
[5] Growing degree days during growing period.
[6] Range of flowering time of durum NAM population grown in the experiment, expressed as days to flowering.
[7] Data is not available.
[8] Mean yield of all genotypic BLUEs.
[9] Number of durum NAM lines and parents.
[10] Spike length measured in cm.
[11] Spike number per unit area.
[12] Canopy related traits include NDVI, and fractional green canopy cover at multiple time points at population level, and tiller number measured on 11 selected genotypes.

[13] Plant height measured in cm.

Table 2. Description of durum wheat genotypes in the 2020 field trial, including the 10 NAM parents and subset of 299 NAM lines

NAM Parent	Pedigree	No. of rep
Fastoz2	T.polonicumTurkeyIG45272/6/ICAMORTA0463/5/Mra1/4/Aus1/3/Scar/GdoVZ579//Bit	2
Fastoz3	Msbl1//Awl2/Bit/3/T.dicoccoidesSYRIG117887	5
Fastoz6	Azeghar1/6/Zna1/5/Awl1/4/Ruff//Jo/Cr/3/F9.3/7/Azeghar1//Msbl1/Quarmal	2
Fastoz7	CandocrossH25/Ysf1//CM829/CandocrossH25	2
Fastoz8	MorlF38//Bcrch1/Kund1149/3/Bicrederaa1/Miki = Kunmiki	3
Fastoz10	Younes/TdicoAlpCol//Korifla = Trouve	1
Fadda98	Awl2/Bit = Awalbit9	5
DBA Aurora	Tamaroi*2/Kalka//RH920318/Kalka///Kalka*2/Tamaroi	3
Jandaroi	110780/111587	1
Outrob4	Ouassel-1/4/GdoVZ 512/Cit//Ruff/Fg/3/Pin/Gre//Trob = Fadda98	1
NAM family	**Pedigree**	**No. of geno**
1	DBA Aurora/Fastoz7	20
2	DBA Aurora/Outrob4	74
3	DBA Aurora/Fastoz8	80
5	DBA Aurora/Fastoz3	80
6	Jandaroi/Fastoz8	16
10	Jandaroi/Outrob4	29

Table 3. Summary statistics for traits studied in the 2020 field trial, including minimum (Min), mean, maximum (Max), and coefficient of variation (CV) for trait BLUEs.

Traits	Min	Mean	Max	CV (%)
NDVI_22DAS[1]	0.22	0.27	0.33	6.3
NDVI_29DAS	0.23	0.33	0.4	9.3
NDVI_36DAS	0.26	0.45	0.55	9.6
NDVI_43DAS	0.39	0.63	0.74	7.9
NDVI_50DAS	0.67	0.84	0.88	3.5
NDVI_63DAS	0.82	0.88	0.9	1.3
NDVI_70DAS	0.87	0.89	0.91	0.6
NDVI_78DAS	0.88	0.9	0.91	0.5
FGCC_29DAS[2]	3.21	10.35	16.52	17.1
FGCC_36DAS	7.6	23.34	33.67	16.9
FGCC_43DAS	20.63	44.01	57.51	13.5
FGCC_50DAS	39.81	70.86	83.91	9.9
AUC_SS[3]	3.77	5.6	7.08	7.4
AUC_TL[4]	14.83	20	21.8	5
AUC_SE[5]	15.47	15.98	16.32	0.7
AUC_VS[6]	34.99	41.57	44.46	3.4
PH (cm)	58	77	94	7.9
DTF (days)	90	95	104	2.1
SL (cm)	7.19	9.21	11.35	8.3
SN (-m^{-2})	115	248	365	17.7
Yld (t-ha^{-1})	1.66	3.63	5.56	17.8

[1] Normalized difference vegetation index (NDVI) measured at 22 days after sowing (DAS).
[2] Fractional green canopy cover (FGCC) measured at 29 DAS.
[3] Area under the curve of smoothed time-series NDVI (AUC) between 0-30 DAS.
[4] AUC between 30-60 DAS.
[5] AUC between 60-78 DAS.

[6] AUC between 0 and 78 DAS.

Table 4. Summary of results from association mapping of canopy development and other traits in the 2020 field trial (2020_WW).

Trait	SNP	Positive allele	Chr[1]	MAF[2]	Pos.St (bp)[3]	Pos.End (bp)[4]	-log10 (*p*)[5]	-log10(*p*-FDR)[6]
NDVI_29DAS	1271404	1	2A	0.21	745108704	745108769	6.15	2.44
	3023448	1	3A	0.49	41109698	41109735	4.80	1.78
	5324123	1	4A	0.13	642498972	642499004	4.33	1.39
	1202152	0	4B	0.49	565602357	565602424	5.72	2.31
	4404447	1	6A	0.35	12144868	12144909	4.97	1.85
	1127685	0	6B	0.22	135162876	135162808	5.09	1.85
NDVI_36DAS	977411	1	4A	0.21	695150339	695150395	5.45	2.03
	1130263	0	5A	0.06	417840038	417840097	7.77	4.05
NDVI_43DAS	1271404	1	2A	0.21	745108704	745108769	5.97	2.25
NDVI_50DAS	2256343	1	2A	0.11	36364366	36364298	5.98	2.57
	1271404	1	2A	0.21	745108704	745108769	6.34	2.63
	3949783	0	2B	0.28	697623388	697623452	4.71	1.47
NDVI_70DAS	996714	1	7A	0.17	109908919	109908968	5.71	2.00
AUC_SS	4004899	1	2A	0.35	735922887	735922955	4.47	1.35
	1095539	1	2B	0.29	618076302	618076370	7.17	3.45
	3946360	1	4A	0.19	24099524	24099564	5.46	2.22
	1093322	0	5B	0.20	528696884	528696822	5.91	2.49
AUC_TL	1271404	1	2A	0.21	745108704	745108769	5.48	1.76
AUC_SE	4004899	1	2A	0.35	735922887	735922955	4.47	1.35
	1095539	0	2B	0.29	618076302	618076370	7.17	3.45
	3946360	1	4A	0.19	24099524	24099564	5.46	2.22
	1093322	0	5B	0.20	528696884	528696822	5.91	2.49

AUC_VS	1271404	1	2A	0.21	745108704	745108769	5.82	2.31
	1108975	0	2B	0.07	55930502	55930570	5.73	2.31
DTF	2256343	0	2A	0.11	36364298	36364366	17.50	13.78
PH	4009205	0	2A	0.27	982116	982183	4.73	1.54
	1698984	1	2A	0.22	131154183	131154248	4.50	1.54
	1017668	1	2A	0.17	695473023	695473091	4.50	1.54
	1088708	1	4B	0.50	637884852	637884784	5.30	1.58
	3064427	1	5B	0.18	533724323	533724367	4.80	1.54
	5411254	0	7A	0.20	32647340	32647399	4.48	1.54
SL	1215020	0	1B	0.47	640187467	640187527	4.65	1.78
	4992547	0	3A	0.22	618058814	618058882	5.86	2.75
	1091678	1	4A	0.46	636321605	636321665	8.84	5.13
	3954609	0	4A	0.12	190565472	190565511	4.67	1.78
	1055097	0	5A	0.09	639650884	639650944	6.51	3.27
	982085	0	5A	0.46	43161899	43161953	4.79	1.78
	1092206	1	6A	0.39	543489106	543489174	7.16	3.75

[1] Chromosome.
[2] Minor allele frequency.
[3] The start of the SNP position on the 'Svevo' durum reference genome.
[4] The end of the SNP position on the 'Svevo' durum reference genome.
[5] -log10 of uncorrected *p* value of marker-trait association.
[6] -log10 of FDR adjusted *p* value.

Table 5. Summary of marker × environment interactions for yield. Predicted means of yield are presented for allele 0 and 1 at each SNP locus, and each SNP allele × trial combination. Significant differences are indicated by different letters at 0.01 probability level following Tukey's test.

Chromosome	2A	2A	2B	2B	2B	3A	4A	6A	6B
Allele	1271404	4004899	1108975	1095539	3949783	3023448	5324123	4404447	1127685

SNP		0	3.24	3.65	3.69	3.63	3.63	3.62	3.7	3.7	3.68
		1	3.77	3.7	3.66	3.76	3.77	3.64	3.58	3.5	3.66
SNP × Env	2017_RW	0	3.43b	3.94c	4c	3.84bc	3.85cd	4.02c	3.93d	4.03c	4.00c
		1	4.00b	3.95c	3.55abcd	4.07c	4.08d	3.80bc	3.98d	3.61b	3.76bc
	2017_WW	0	4.5bc	4.95d	4.91d	4.70d	4.71e	4.81d	4.96e	4.98d	4.88d
		1	5.11c	4.9d	4.67bcd	5.16e	5.16f	4.86d	4.83e	4.58d	5.05d
	2019_TS	0	1.86a	2.22a	2.27a	2.26a	2.26a	2.25a	2.20a	2.26a	2.26a
		1	2.22a	2.25a	2.45abc	2.22a	2.22a	2.22a	2.35a	2.05a	2.11a
	2020_WW	0	3.19b	3.49b	3.57b	3.70b	3.72bc	3.40b	3.69c	3.54b	3.60b
		1	3.74b	3.69bc	3.98bcd	3.60b	3.59b	3.68bc	3.16b	3.76b	3.74bc
p-value	Main effect		1.36e-05	0.1	0.66	0.22	0.28	0.13	0.07	0.52	0.93
	M × E effect		0.02	0.04	4.39e-09	8.64e-06	8.93e-06	0.01	4.47e-06	1.22e-08	0.002

Table 6. Comparison of two homozygous alleles at four SNP loci for spike traits measured in 2017_WW and 2020_WW. Data was analysed with unpaired t-test in two trials separately.

SNP	Chr	Trial	Allele	N[1]	Mean _SL[2]	*p*-value_SL	Mean_SN[3]	*p*-value_SN
1095539	2B	2017_WW	0	80	7.29	<0.05	323	0.16
			1	66	7.52		311	
		2020_WW	0	89	8.98	<0.001	254	0.11
			1	218	9.3		245	
3949783	2B	2017_WW	0	80	7.35	0.35	321	0.40
			1	66	7.46		314	
		2020_WW	0	84	8.99	<0.001	248	0.94
			1	223	9.31		248	
5324123	4A	2017_WW	0	92	7.44	0.44	311	<0.05
			1	50	7.34		330	

4404447	6A	2020_WW	0	256	9.27	<0.001	245	<0.01
			1	36	8.82		268	
		2017_WW	0	122	7.39	0.37	321	0.12
			1	25	7.46		304	
		2020_WW	0	200	9.18	0.28	250	0.27
			1	109	9.28		244	

[1] Number of individuals carrying allele 0 or 1 of a given SNP within the trial.
[2] Mean spike length (cm).
[3] Mean spike number per m^2.

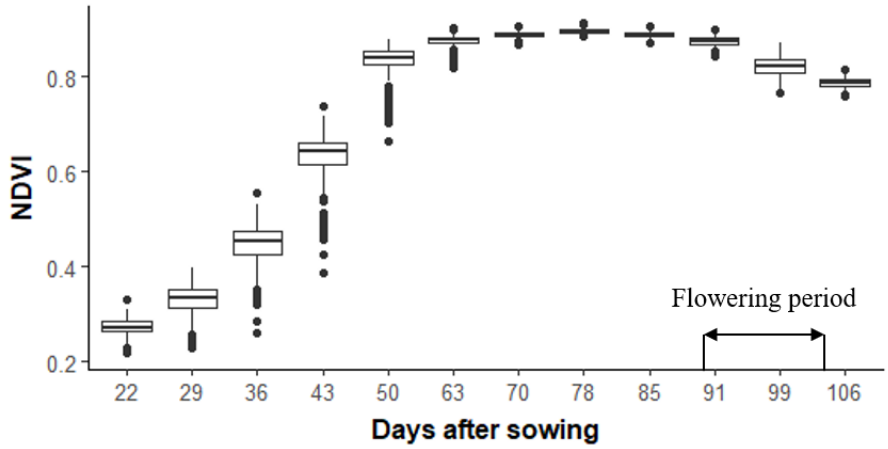

Fig. 1. Variability of normalized difference vegetation index (NDVI) of the durum nested-association mapping population in 2020_WW. Each boxplot represents the range of best linear unbiased estimates (BLUEs) for NDVI at each time-point.

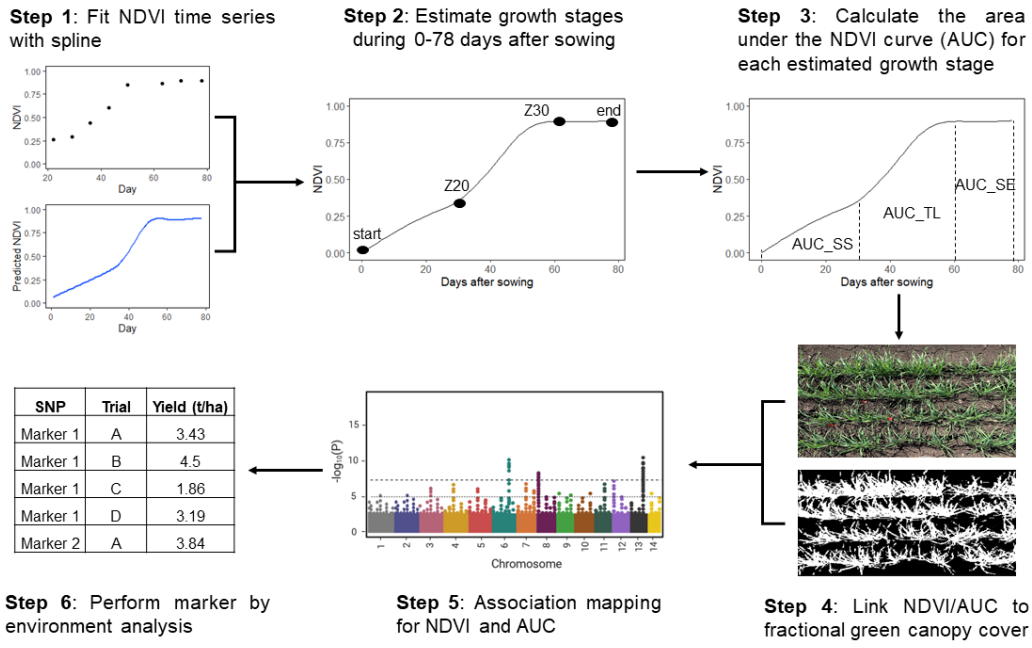

Fig. 2. Experimental analyses performed in this study involved the fitting of NDVI time series with a spline (1), estimation of growth stages (2), calculation of AUC for NDVI (3), link of NDVI/AUC to fractional green canopy cover (4), association mapping (5) and marker by environment analysis (6).

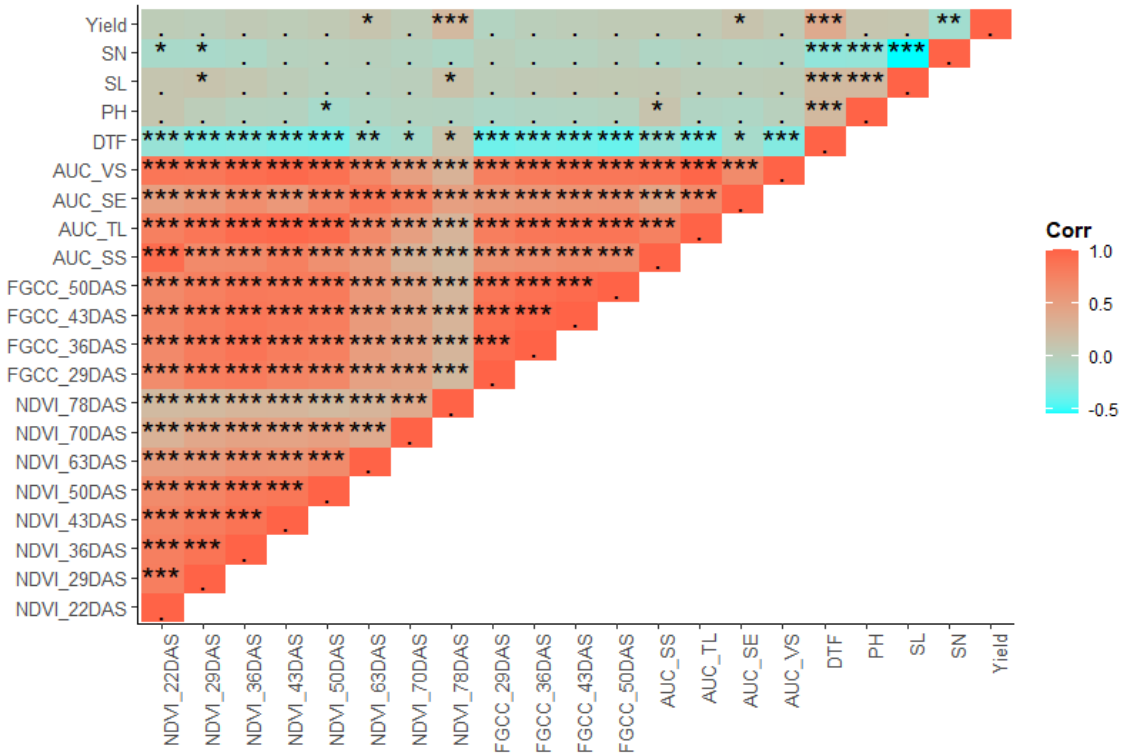

Fig. 3. Heatmap of trait by trait correlations in the 2020_WW trial. Pearson's correlation was computed for each pair of traits. The colour key represents the Pearson's correlation coefficient. Level of significance *: $p < 0.05$; **: $p < 0.01$; ***: $p < 0.001$. The explanation for trait abbreviation can be found in Table 3.

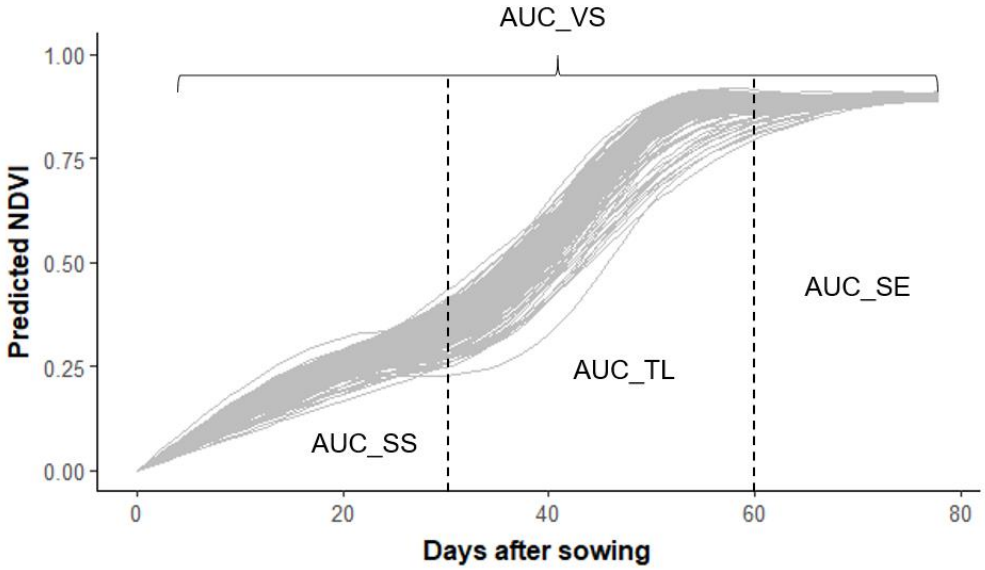

Fig. 4. Trajectories of time-series NDVI of all genotypes in the mapping population fitted with smoothing splines. The breakpoints 30 and 60 days after sowing were used to bin the whole range of simulated NDVI data. First phase = seedling stage (AUC_SS, 0-30 DAS), second phase = tillering (AUC_TL, 30-60 DAS), third phase = stem elongation (AUC_SE, 60-78 DAS).

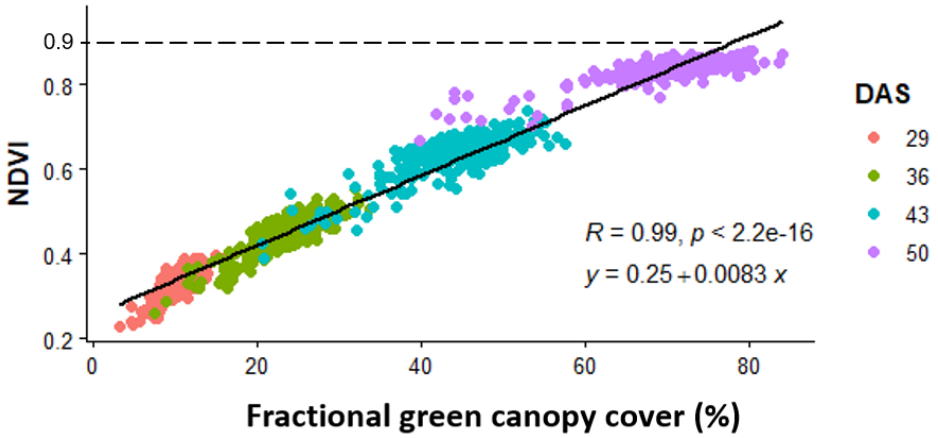

Fig. 5. Relationship between BLUEs of NDVI and fractional green canopy cover measured at 29, 36, 43 and 50 DAS.